

# NEW PERIODIC SOLUTIONS IN THE AIRCRAFT MAXIMUM RANGE PROBLEM

**A.E. Sagalakov and A.S. Filatyev**  
**Central Aerohydrodynamic Institute (TsAGI)**

**Keywords:** *maximum principle, maximum range problem, oscillatory trajectory*

## Abstract

*The classical problem of maximization of the aircraft range is considered. The solution is based on using the Pontryagin maximum principle. New analytical solutions are obtained within a framework of the approximate pseudo-conservative model of the motion. Realizability and efficiency of the obtained optimal oscillatory trajectories are shown in comparison with the traditional steady cruise flight.*

## 1 Introduction

The maximum range problem is a classical problem in aircraft design. Traditionally, an airplane trajectory consists of three main segments: the climb, cruise flight at nearly constant altitude and descent to a landing point. The cruise is the longest and well-studied phase of flight. Therefore, the optimization problem for cruise flight has become a subject of authors' interest.

The aim of this paper is to present the obtained qualitative results of the problem study on the base of the Pontryagin maximum principle [1], including investigation of the optimal control law, especially alternative to the traditional steady solution, and its dependences on the functional, constraints and other parameters of the problem.

The principal feature of this optimization problem is possible degeneration with increasing the flight duration as local changes of control variables (the angle of attack and thrust) have a weak influence on distant trajectory sections and the functional.

Usually, some simplifications are introduced into equations of motion to overcome this difficulty.

One of the most often used simplification for the cruise phase is the hypothesis of quasi-stationarity [2]:

$$\gamma \approx 0, \dot{\gamma} \approx 0, \quad (1.1)$$

where  $\gamma$  is the path angle and  $\dot{\gamma}$  is its time-derivative. The range  $x$  of the level flight is defined by the Breguet formula [3]:

$$x = \left( \frac{Kv}{c_e} \right) \ln \frac{m_i}{m_f}, \quad (1.2)$$

where  $K$  is the lift-to-drag ratio,  $v$  is the velocity,  $c_e$  is the specific fuel mass consumption,  $m$  is the mass, sub-indexes “ $i$ ” and “ $f$ ” correspond to initial and final points. From (1.2) the well-known result follows about the optimality of the cruise flight at the maximum of expression  $\left( \frac{Kv}{c_e} \right)$ .

The cruise minimum fuel consumption problem at constant altitude and fixed-time flight is considered in [4]. This is a mutual problem with relation to the maximum range problem at fixed mass consumption. The thrust is taken as a control variable. The problem is solved using the Pontryagin maximum principle. By calculation for this problem authors demonstrate the existence of a singular arc for the optimal thrust control.

A qualitative analysis of the maximum range problem is performed in [5]. The problem is solved by the energy approach, where altitude and thrust are taken as control variables. There are considered two statements: for a given fuel

consumption with free flight time and for given flight time with free fuel consumption.

Speyer seems to be the first [6] who doubted reasonably about optimality of the steady level flight in the considered problem and proved that it fails the optimality conditions in terms of classical calculus variations. It was also shown that the oscillatory trajectory can reduce the fuel consumption when compared with the level flight.

The minimum fuel consumption problem of subsonic aircraft with constant mass by using an oscillatory trajectory is considered in [7]. The boundary conditions imply the equality of initial and final velocity and altitude. The problem is solved by selection of parameters of a sine law for altitude changes. On the basis of numeric calculations authors show the existence of such oscillatory trajectories that give the less fuel mass consumption as compared with the level flight.

Shepard and Bilimoria [8] considered the problem of minimizing both the fuel mass consumption  $\Delta m_f$  and time of flight  $\tau$  by introducing the penalty function:

$$\Phi = (\eta\tau + \Delta m_f).$$

In the model the following simplifications, which correspond to the conditions of stationary flight, are made: the weight equals the lift and the drag equals the thrust. The velocity and altitude are taken as the control variables. The problem is solved by using the Pontryagin maximum principle. It is shown that increasing the penalty factor  $\eta$ , i.e. a relative rise of a role of the time in comparison with the mass, the average velocity increases at the optimal trajectory, and the average altitude first increases and then decreases.

In [9] authors minimize the fuel mass consumption and flight time for the functional that is similar to [8]:

$$\Phi = \frac{1}{x_f} \int_0^{x_f} \frac{\eta + \chi c_e T}{v \cos \gamma} dx \Rightarrow \min ,$$

where  $\eta, \chi$  are actually the penalty factors. The initial and final velocity and altitude are considered as equal. Thrust and lift coefficient

are taken as control variables. Aircraft is considered as a point with a constant mass. The problem is solved by using the Pontryagin maximum principle. By calculation for different values of  $\eta, \chi$  periodic solutions are shown with singular arc and bang-bang control.

A more detailed overview of fundamental results on this topic can be found, for example, in [10], [11].

In contrast to the above mentioned works in this paper a priori assumption (1.1) of the quasi-stationary character of motion is not used and  $\gamma$  and  $\dot{\gamma}$  may be arbitrary. The path angle  $\gamma$  is considered as the control variable without any constraints. The analytical optimal solutions are obtained in the framework of the approximate pseudo-conservative motion model. It is shown that the solutions have oscillatory character that gives gain in the range in comparison with the level flight. Then, generalizations of the problem are considered with constraints on the velocity, altitude and fuel mass consumption. The optimization problem with the last constraint is solved numerically using the continuation method. Finally, the obtained approximate analytical optimal solutions are tested on the more comprehensive model of the motion for typical maneuverable aircraft. Their good agreement on the functional and efficiency of the oscillatory trajectories in comparison with the traditional level cruise flight are demonstrated.

## 2 Problem statement

Consider the aircraft maximum range problem. Movement of aircraft is considered in a flat homogeneous gravitational field as a mass point, which is described by following equations:

$$\begin{aligned}
 \dot{v} &= \frac{T-D}{m} - g \sin \gamma, \\
 \dot{\gamma} &= \frac{L}{mv} - \frac{g \cos \gamma}{v}, \\
 \dot{h} &= v \sin \gamma, \\
 \dot{x} &= v \cos \gamma, \\
 \dot{m} &= -c_e T,
 \end{aligned} \tag{2.1}$$

where  $T$  is the thrust,  $D = c_x q S$  is the aerodynamic drag,  $L = c_y q S$  is the aerodynamic lift,  $g$  is the acceleration of gravity,  $h$  is the altitude,  $c_x$  is the drag coefficient,  $c_y$  is the lift coefficient,  $q$  is the dynamic pressure,  $S$  is the reference area.

Let us use the dimensionless variables:

$$\begin{aligned}
 h &= \left( \frac{h}{R} \right)_{\text{dim}}, \quad v = \frac{v_{\text{dim}}}{\sqrt{(g_0 R)_{\text{dim}}}}, \\
 t &= t_{\text{dim}} \sqrt{\left( \frac{g_0}{R} \right)_{\text{dim}}}, \quad m = \left( \frac{m}{m_i} \right)_{\text{dim}}, \\
 T &= \left( \frac{T}{m_i g_0} \right)_{\text{dim}}, \quad D = \left( \frac{D}{m_i g_0} \right)_{\text{dim}}, \\
 L &= \left( \frac{L}{m_i g_0} \right)_{\text{dim}}, \quad x = \left( \frac{x}{R} \right)_{\text{dim}},
 \end{aligned} \tag{2.2}$$

where the index «dim» designates dimensional variables,  $g_0$  is the gravity acceleration at sea level,  $R$  is the average radius of the Earth,  $m_i$  is the initial mass of aircraft.

Then, equations (2.1) take the form:

$$\begin{aligned}
 \dot{v} &= \frac{T-D}{m} - \sin \gamma, \\
 \dot{\gamma} &= \frac{L}{mv} - \frac{\cos \gamma}{v}, \\
 \dot{h} &= v \sin \gamma, \\
 \dot{x} &= v \cos \gamma, \\
 \dot{m} &= -c_e T.
 \end{aligned} \tag{2.3}$$

Due to the mass is slowly changing variable, we follow for the many previous works, including mentioned above, and neglect the influence of mass changes in the right sides of (2.3).

Because  $\gamma$  is the rapidly changing variable in comparison with  $v$ ,  $h$  and  $x$ , it is convenient to take  $\gamma$  as the control variable and to rule out the differential equation for  $\gamma$ .

Let us introduce new phase coordinates as follows:  $w$  is the pseudo-velocity,  $\nu$  is the pseudo-path angle, which are associated with the initial variables by the following relationships:

$$\begin{aligned}
 |w| &= v, \\
 w \cos \nu &= v \cos \gamma, \\
 w \sin \nu &= v \sin \gamma.
 \end{aligned}$$

Note that the pseudo-velocity can take negative values, and the pseudo-path angle may differ from  $\gamma$  by  $180^\circ$ .

For brevity, below we omit the word "pseudo" in names of the new variables where it cannot lead to misunderstandings.

The system (2.3) with the new variables takes the form:

$$\begin{aligned}
 \dot{w} &= T - D - \sin \nu, \\
 \dot{h} &= w \sin \nu, \\
 \dot{x} &= w \cos \nu.
 \end{aligned} \tag{2.4}$$

We use the following boundary conditions. At the initial time  $t_i=0$ :

$$w(t_i) = w_i, h(t_i) = h_i, x(t_i) = 0. \tag{2.5}$$

At the final time  $t_f$ :

$$t_f = f(x), w(t_f) = w_i, h(t_f) = h_i. \tag{2.6}$$

Equality of  $v$  and  $h$  at the beginning (2.5) and end (2.6) of the trajectory does not matter, but in this work it allows to consider the level flight as one of the possible solution and compare it with the optimal solutions obtained.

The performance criterion is the range:

$$\Phi \equiv x(t_f) \Rightarrow \max_{\{v\}}. \tag{2.7}$$

### 3 Optimality conditions

According to the maximum principle [1] the optimal control is determined from the condition:

$$v_{opt}(t) = \operatorname{argmax} H, \quad (3.1)$$

where  $H = \boldsymbol{\lambda}^T \mathbf{f}$  is the Hamiltonian of (2.4),  $\mathbf{f}$  is the vector of the right sides of equations (2.4),  $\boldsymbol{\lambda}^T = \{\lambda_w, \lambda_h, \lambda_x\}$  is the vector of conjugate variables corresponding to the variables of the phase vector  $\mathbf{x} = \{w, h, x\}$  and satisfies the equation:

$$\dot{\boldsymbol{\lambda}} = - \left( \frac{\partial H}{\partial \mathbf{x}} \right)^T. \quad (3.2)$$

Taking into account (2.4) and (3.2) we obtain:

$$\begin{aligned} \dot{\lambda}_w &= - \frac{\partial H}{\partial w} = -\lambda_h \sin \nu - \lambda_x \cos \nu - \lambda_w \frac{\partial(T-D)}{\partial w}, \\ \dot{\lambda}_h &= - \frac{\partial H}{\partial h} = -\lambda_w \frac{\partial(T-D)}{\partial h}, \\ \dot{\lambda}_x &= - \frac{\partial H}{\partial x} = 0. \end{aligned} \quad (3.3)$$

The transversality conditions are [12]:

$$(\delta \Phi - H \delta t + \boldsymbol{\lambda} \delta \mathbf{x}) \Big|_{t_f}^{t_i} = 0, \quad (3.4)$$

where variations are taken on admissible variety. For (3.3), (3.4) the transversality conditions are reduced to one condition on the right end of the trajectory:

$$\lambda_x(t_f) = 1. \quad (3.5)$$

To determine the optimal control  $v_{opt}$  let us select a part  $H^v$  of the Hamiltonian that is clearly dependent on the control:

$$H^v = (\lambda_h w - \lambda_w) \sin \nu + w \cos \nu. \quad (3.6)$$

From (3.1) and (3.6) we obtain the optimal control law:

$$\sin v_{opt} = \frac{A}{\sqrt{A^2 + w^2}}, \quad \cos v_{opt} = \frac{w}{\sqrt{A^2 + w^2}}, \quad (3.7)$$

where  $A = \lambda_h w - \lambda_w$ .

Five phase conditions (2.5) and (2.6) at the boundary points and one transversality condition (3.5) enclose boundary value problem for the system of six differential equations (2.4) and (3.3). Thus, the Pontryagin maximum principle allows to reduce the original

optimization problem in the functional space to the boundary value problem: it is required to find three values  $\lambda_w, \lambda_x, \lambda_h$  on the left end, so to satisfy three conditions (2.6) and (3.5) on the right end of the trajectory.

The phase system (2.4) is autonomous, so the first integral takes place at the optimal control:

$$H \Big|_{v_{opt}} = \text{const}. \quad (3.8)$$

Note that the same integral holds at a constant control:

$$H \Big|_{v=\text{const}} = \text{const}. \quad (3.9)$$

The property (3.9), as was shown in [12], is useful for verification of a mathematical model of an optimization software package (more details on this subject will be discussed below in Section 8).

#### 4 Analytical solutions for the pseudo-conservative model

Let us make the following assumptions:

- the thrust is equal to the aerodynamic drag,
- on the considered time interval the change of aircraft mass can be neglected to the structure of the optimal control,
- the path angle as a fast variable is taken as the control.

The assumptions are quite appropriate for studying the motion of aircraft with high aerodynamic efficiency. Moreover, the first two assumptions are consistent with the quasistationary conditions, and the third assumption significantly broadens the class of acceptable trajectories in comparison with quasistationary trajectories because it doesn't confine the path angle  $\nu$ .

After these simplifications, the equations (2.4) take the form:

$$\begin{aligned} \dot{w} &= -\sin \nu, \\ \dot{h} &= w \sin \nu, \\ \dot{x} &= w \cos \nu. \end{aligned} \quad (4.1)$$

The Hamiltonian for (4.1) is:

$$H = -\lambda_w \sin \nu + \lambda_h w \sin \nu + \lambda_x w \cos \nu. \quad (4.2)$$

According to (3.2) (4.2) the conjugate system is:

$$\begin{cases} \dot{\lambda}_w = -\lambda_h \sin \nu - \lambda_x \cos \nu, \\ \dot{\lambda}_h = 0, \\ \dot{\lambda}_x = 0. \end{cases} \quad (4.3)$$

From (4.3) we obtain the following solutions:

$$\lambda_h = const, \lambda_x = const, \quad (4.4)$$

and due to the transversality condition (3.5):

$$\lambda_x \equiv 1. \quad (4.5)$$

According to (3.1):

$$\begin{aligned} \sin \nu_{opt} &= \frac{\lambda_h w - \lambda_w}{\sqrt{(\lambda_h w - \lambda_w)^2 + w^2}}, \\ \cos \nu_{opt} &= \frac{w}{\sqrt{(\lambda_h w - \lambda_w)^2 + w^2}}. \end{aligned} \quad (4.6)$$

Substituting (4.6) in (4.2) and taking into account (3.8), we obtain for the optimal trajectory:

$$H = \sqrt{(\lambda_h w - \lambda_w)^2 + w^2} = const > 0. \quad (4.7)$$

Substituting (4.6) in (4.3) and (4.1) and taking into account (4.7), we obtain:

$$\begin{cases} \dot{\lambda}_w = -\frac{1 + \lambda_h^2}{H} w + \frac{\lambda_h}{H} \lambda_w, \\ \dot{w} = -\frac{\lambda_h}{H} w + \frac{1}{H} \lambda_w. \end{cases} \quad (4.8)$$

Differentiating the second equation in (4.8) and substituting it into the first equation of (4.8) with (4.4) and (4.7), it results in:

$$\ddot{w} + \frac{w}{H} = 0. \quad (4.9)$$

The equation (4.9) has the solution:

$$w = C_1 \sin\left(\frac{t}{H}\right) + C_2 \cos\left(\frac{t}{H}\right), \quad (4.10)$$

where the constants  $C_1, C_2$  are determined from the boundary conditions (2.5) and (2.6).

Substituting (4.10) into (4.8), we obtain:

$$\lambda_w = C_1 \cos\left(\frac{t}{H}\right) - C_2 \sin\left(\frac{t}{H}\right). \quad (4.11)$$

The optimal control (4.6) with (4.10) and (4.11) takes the form:

$$\begin{aligned} \sin \nu_{opt} &= \frac{C_2}{H} \sin\left(\frac{t}{H}\right) - \frac{C_1}{H} \cos\left(\frac{t}{H}\right), \\ \cos \nu_{opt} &= \frac{w(t)}{H}. \end{aligned} \quad (4.12)$$

The Hamiltonian by substituting (4.7) into (4.10) - (4.12) takes the form:

$$H = \sqrt{C_1^2 + C_2^2} = const. \quad (4.13)$$

For  $C_1, C_2$  we have the conditions:

$$C_1 \sin\left(\frac{t_f}{H}\right) = w_i \left(1 - \cos\left(\frac{t_f}{H}\right)\right), \quad C_2 = w_i. \quad (4.14)$$

Consider the case  $\frac{t_f}{H} = 2\pi n$ , where  $n$  is integer. Then, from (4.13) and (4.14):

$$C_1 = \pm \sqrt{H^2 - w_i^2}. \quad (4.15)$$

If  $\frac{t_f}{H} \neq 2\pi n$ , from (4.14):

$$C_1 = \frac{w_i \left(1 - \cos\left(\frac{t_f}{H}\right)\right)}{\sin\left(\frac{t_f}{H}\right)}. \quad (4.16)$$

Substituting  $\sin \nu, \cos \nu$  from (4.12) into the equality:

$$\frac{d}{dt}(\sin \nu) = \cos \nu \frac{d\nu}{dt},$$

and taking the derivative of  $\sin \nu$  it is obtained:

$$\frac{d\nu}{dt} = \frac{1}{H}. \quad (14.7)$$

So the optimal pseudo-path angle has linear dependence from time:

$$v = v_i + \frac{1}{H}t. \quad (14.8)$$

### 5 Analysis of optimal oscillatory solutions

According to (4.10) the optimal trajectories are periodic oscillatory. The local extremals (satisfying necessary optimality conditions of the maximum principle) are not unique and their quantity is determined by the quantity of solutions of following equations for  $H, C_1$ :

$$\begin{cases} H = \sqrt{C_1^2 + w_i^2}, \\ w_i = C_1 \sin\left(\frac{t_f}{H}\right) + w_i \cos\left(\frac{t_f}{H}\right). \end{cases} \quad (5.1)$$

A part of the solutions (5.1) is obvious, they are written in the form:

$$H = \frac{t_f}{2\pi n}, \quad (5.2)$$

where  $n$  is integer. The quantity of solutions with (5.1) and (5.2):

$$N < \left\lceil \frac{t_f}{2\pi w_i} \right\rceil, \quad (5.3)$$

where  $[f]$  is the nearest to  $f$  integer not exceeding  $f$ .

The other solutions are obtain from:

$$H = \sqrt{w_i^2 \tan^2\left(\frac{t_f}{2H}\right) + w_i^2} = \left| \frac{w_i}{\cos\left(\frac{t_f}{2H}\right)} \right|. \quad (5.4)$$

Equation (5.4) has the following geometric interpretation (Fig. 1). The quantity of intersections of the line  $y = \pm w_i x$  with the function  $y = \cos(0.5t_f x)$ , where  $x = 1/H$ , corresponds to the quantity of solutions of (5.4). Angle of the slope is directly proportional to  $w_i$  and when it increases the quantity of solutions decreases. The oscillation frequency is directly proportional to  $t_f$  and when it increases the quantity of solutions increases too.

The (5.1) shows that the local extremals depend on  $w_i$  and time of flight  $\tau = t_f t_i$ . The

relative change of the functional  $\Delta \bar{x} = \frac{x_{opt} - x_{hor}}{x_{hor}}$ , where  $x_{hor} = w_i \tau$  is determined

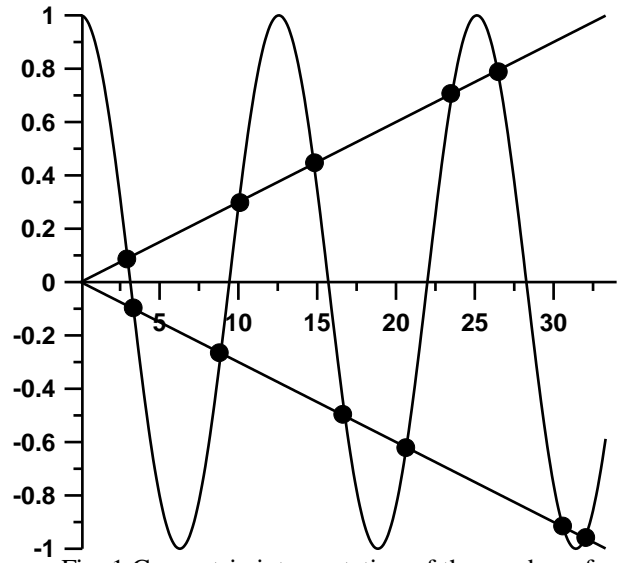


Fig. 1 Geometric interpretation of the number of solutions

by a change of the generalized parameter  $\frac{\tau}{w_i}$ .

Fig. 2 shows the dependencies  $\Delta \bar{x} \left( \frac{\tau}{w_i} \right)$  for different extremals. As can be seen from Fig. 2,  $\Delta \bar{x}$  increases with increasing  $\tau$  and with decreasing  $w_i$ . In the considered range of the

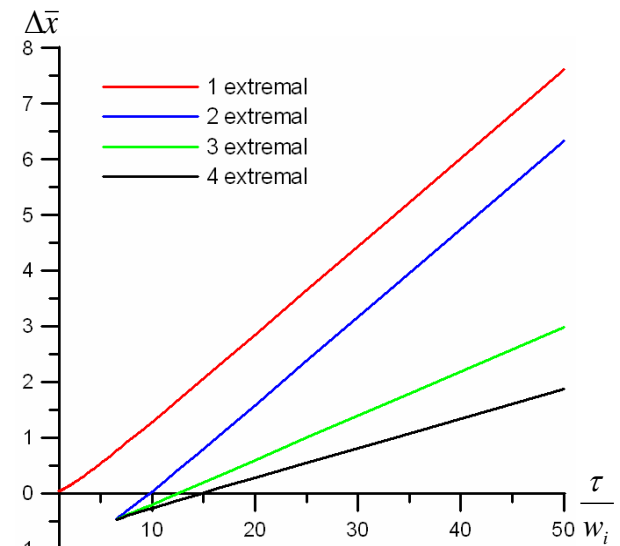


Fig. 2 Dependence of relative increment of range from generalized parameter.

parameter  $\frac{\tau}{w_i}$  the first extremal always has the

gain in the functional as compared with the level flight.

The solutions are demonstrated on the example with following parameter values:

$$w_i = 240 \frac{m}{s}, \tau = 800s. \quad (5.5)$$

As it can be seen from Fig. 3, the optimal periodic trajectories have almost five-fold flight range advantage in comparison with the level cruise. Total in case (5.5), there are 16 local extremals. Seven of them have the advantage of the functional under the level flight from 496%

(the extremal no.1) to 18% (no.7). These trajectories are characterized by changes of altitude from 364 km to 7 km (Fig. 4), indicating possible areas of their application: from space and hypersonic vehicles to airplanes. It is obvious that the global extremum delivers the extremal no. 1 only.

### 6. Analytical solution with constraints of velocity and altitude

Consider the maximum range problem with constraint on state variables  $w$  and  $h$  in the pseudo-conservative statement.

The equations of motion coincide with (4.1). We assume the boundary conditions to be (2.5) and (2.6). The control variable is the path angle  $\nu$ .

Firstly consider the constraint on  $w$ :

$$w \leq w_{con}. \quad (6.1)$$

On the constraint arc:

$$\begin{aligned} S_1 = w - w_{con} &= 0, \\ \dot{S}_1 = -\sin \nu &= 0. \end{aligned} \quad (6.2)$$

According to (6.2) the Hamiltonian has the form [14]:

$$H = -\lambda_w \sin \nu + \lambda_h w \sin \nu + \lambda_x w \cos \nu - \mu \sin \nu, \quad (6.3)$$

where  $\mu=0$  beyond the constraint arc.

At the point of entry to the constraint arc  $t_1$  the next condition for the conjugate system and Hamiltonian must be satisfied:

$$\begin{aligned} \lambda_w(t_1^-) &= \lambda_w(t_1^+) + \pi, \\ \lambda_h(t_1^-) &= \lambda_h(t_1^+), \\ \lambda_x(t_1^-) &= \lambda_x(t_1^+), \\ H(t_1^-) &= H(t_1^+). \end{aligned} \quad (6.4)$$

From (4.1) and (6.2) we have the following solution on the constraint arc:

$$\begin{aligned} \nu &= 0, \\ w &= w_{con}. \end{aligned} \quad (6.5)$$

From (6.3) - (6.5) we obtain:

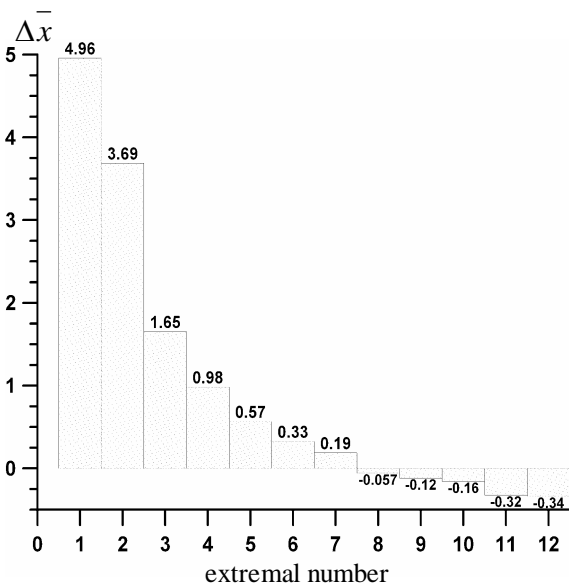


Fig. 3 The relative increment of the range for different extremals

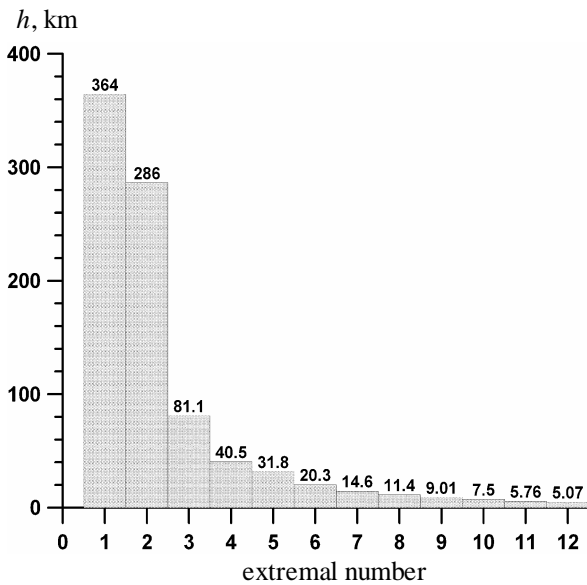


Fig. 4 The altitude change for different extremals

$$H(t_1^-) = H(t_1^+) = H = w_{con}. \quad (6.6)$$

The solution before the constraint arc is obtained from (3.2), (4.1) and (6.3):

$$w = C_1 \sin\left(\frac{t}{w_{con}}\right) + C_2 \cos\left(\frac{t}{w_{con}}\right). \quad (6.7)$$

From (2.5) and (6.5) it is followed:

$$\begin{aligned} t_1 &= w_{con} \arccos\left(\frac{w_i}{w_{con}}\right), \\ C_1 &= w_i \tan\left(\frac{t_1}{w_{con}}\right), \\ C_2 &= w_i. \end{aligned} \quad (6.8)$$

The solution after the constraint arc is obtained from (3.2), (4.1) and (6.3):

$$w = C_3 \sin\left(\frac{t}{w_{con}}\right) + C_4 \cos\left(\frac{t}{w_{con}}\right). \quad (6.9)$$

From (2.6) and (6.5) it is resulted in:

$$\begin{aligned} t_2 &= t_f - w_{con} \arccos\left(\frac{w_i}{w_{con}}\right), \\ C_4 &= w_{con} \cos\left(\frac{t_2}{w_{con}}\right), \\ C_3 &= w_{con} \sin\left(\frac{t_2}{w_{con}}\right). \end{aligned} \quad (6.10)$$

Now, consider the constraint on  $h$ :

$$h \leq h_{con}. \quad (6.11)$$

On the constraint arc:

$$\begin{aligned} S_2 &= h - h_{con} = 0, \\ \dot{S}_2 &= w \sin \nu = 0. \end{aligned} \quad (6.12)$$

The Hamiltonian has the form:

$$H = (-\lambda_w + \lambda_h w + \mu w) \sin \nu + \lambda_x w \cos \nu, \quad (6.13)$$

where  $\mu=0$  beyond the constraint arc.

At the point of entry to the constraint arc  $t_1$  the next condition for the conjugate system and the Hamiltonian must be satisfied:

$$\begin{aligned} \lambda_w(t_1^-) &= \lambda_w(t_1^+), \\ \lambda_h(t_1^-) &= \lambda_h(t_1^+) + \pi, \\ \lambda_x(t_1^-) &= \lambda_x(t_1^+), \\ H(t_1^-) &= H(t_1^+). \end{aligned} \quad (6.14)$$

From (4.1) and (6.12) we have the following solution on the constraint arc:

$$\begin{aligned} \nu &= 0, \\ w &= w_h = \sqrt{2(h_i - h_{con}) + w_i^2}, \\ h &= h_{con}, \end{aligned} \quad (6.15)$$

where  $w_h$  is the velocity at the constraint arc.

From (6.13), (6.14) and (6.15) we obtain:

$$H(t_1^-) = H(t_1^+) = H = w_h. \quad (6.16)$$

The solution before the constraint arc is followed from (3.2), (4.1) and (6.13):

$$\begin{aligned} w &= C_1 \sin\left(\frac{t}{w_h}\right) + C_2 \cos\left(\frac{t}{w_h}\right), \\ h &= \frac{w_i^2}{2} + h_i - \frac{w^2}{2}. \end{aligned} \quad (6.17)$$

From (2.5) and (6.15) we obtain:

$$\begin{aligned} t_1 &= w_h \arccos\left(\frac{w_i}{w_h}\right), \\ C_1 &= w_i \tan\left(\frac{t_1}{w_h}\right), \\ C_2 &= w_i. \end{aligned} \quad (6.18)$$

The solution after the constraint arc is obtained from (3.2), (4.1) and (6.15):

$$\begin{aligned} w &= C_3 \sin\left(\frac{t}{w_h}\right) + C_4 \cos\left(\frac{t}{w_h}\right), \\ h &= \frac{w_i^2}{2} + h_i - \frac{w^2}{2}. \end{aligned} \quad (6.19)$$

From (2.6) and (6.15) it is resulted in:

$$\begin{aligned}
 t_2 &= t_f - w_h \arccos\left(\frac{w_i}{w_h}\right), \\
 C_4 &= w_h \cos\left(\frac{t_2}{w_h}\right), \\
 C_3 &= w_h \sin\left(\frac{t_2}{w_h}\right).
 \end{aligned} \tag{6.20}$$

**7. Statement of the problem with constraint on fuel mass consumption**

Consider the maximum range problem in pseudo-conservative statement (4.1) taking into account the fuel mass constraint:

$$m_i - m_f = \Delta m,$$

where  $\Delta m$  is the given mass of fuel consumed. The equations of motion take the form:

$$\begin{aligned}
 \dot{w} &= -\sin \nu, \\
 \dot{h} &= w \sin \nu, \\
 \dot{x} &= w \cos \nu, \\
 \dot{m} &= -c_e T.
 \end{aligned} \tag{7.1}$$

According to the assumption  $T=D$  the equation for the mass in (7.1) takes the form:

$$\dot{m} = -c_e D = -B\rho w^2, \tag{7.2}$$

where  $B = 0.5c_e c_x S$ .

The path angle  $\nu$  is the control variable.

We use the following boundary conditions.

At the initial time  $t_i$ :

$$w(t_i) = w_i, h(t_i) = h_i, x(t_i) = 0, m(t_i) = m_i. \tag{7.3}$$

At the final time  $t_f$ :

$$t_f = \text{fix}, w(t_f) = w_i, h(t_f) = h_i, m(t_f) = m_f. \tag{7.4}$$

The functional is the range:

$$\Phi \equiv x(t_f) \Rightarrow \max_{\{\nu\}}. \tag{7.5}$$

Note that the problem covers a wide class of mutual problems. These include:

- maximizing the range with a given flight time and a given mass of fuel,

- minimization of flight time with a given range and a given mass of fuel,
- minimization the fuel consumption with a given range and a given flight time.

**8 Accuracy analysis**

One of the important advantages of the Pontryagin maximum principle is a capability to obtain the objective information about correctness of the various parts of the program and the accuracy of calculations. Objective ways to diagnose the correct operation of the basic blocks of the program responsible for the formation of the phase and conjugate systems of

Table 1 Hamiltonian change vs integration step under constant control

$\Delta t$	0.000125	0.00025	0.0005	0.001
$\Delta H$	2.94E-13	2.42E-12	1.95E-11	1.58E-10

equations, the optimal control in the indirect optimization problem are justified in [13]. Using these procedures can not only reliably diagnose the presence of analytical mistakes or programming errors, but also localize them in the program.

Following [13] the integration on a constant control allows to check the correctness of programming the conjugate system. In the numerical integration the Hamiltonian variations along the trajectory at a constant control should be determined only by the integration step, i.e. the method error of numerical integration. In this paper the Runge-Kutta integration method of the 4th order is used. It is characterized by a decrease of one or two orders of magnitude errors keeping the integral (3.9) with decreasing integration step  $\Delta t$  twice [13] (see Table. 1). (This is true only if  $\Delta t$

Table 2 Hamiltonian change vs integration step under optimal control

$\Delta t$	0.000125	0.00025	0.0005	0.001
$\Delta H$	7.19E-8	2.89E-7	1.19E-6	6.18E-6

is not very small and the method error dominates the rounding error [15]).

At the optimal control the Hamiltonian has also to be constant (see (3.9)). A rational choice of the integration step for phase and conjugation

systems of equations can be based on the following condition, which uses the physical meaning of conjugate variables as influence functions of phase variables on the functional and the Hamiltonian meaning as the influence function of time [13]:

$$|\Delta H| \Delta t \approx \Delta \Phi \ll \Phi, \quad (8.1)$$

where  $\Delta H$  is the maximum  $H$ -change at the optimal trajectory, caused by errors of integration with step  $\Delta t$ ,  $\Delta \Phi$  is the given allowable error of the calculation of the maximum flight range. If there is no mistakes in account of optimality conditions the integration step reduction in two times follows to the error reduction of  $H$  in an order (see Table. 2).

### 9 Numerical procedure of BVP solution

Technique of indirect optimization based on the Pontryagin maximum principle is implemented in the program complex "ASTER" [16]. The complex "ASTER" includes:

- The modified Newton method for solving the multipoint boundary value problem. It enables a high-speed convergence of the iterative process of solving the boundary value problem in a neighborhood of the extremum.
- The continuation method and the method of local extremals selection, which regularizes procedure to obtain the optimal solution far from a known solution.

In this paper, the initial solution for the continuation method for solving the problem (7.1) – (7.4) was the analytical solution obtained in the framework of the pseudo-conservative statement described in Section 4. In this case, the homotopy parameter  $\chi = [0, 1]$  is entered as:

$$\Delta m = \chi \Delta m_b + (1 - \chi) \Delta m_a, \quad (9.1)$$

where  $\Delta m$  is the current mass of consumed fuel,  $\Delta m_b$  is the final mass of consumed fuel,  $\Delta m_a$  is the mass of consumed fuel obtained by the analytical solution. In Fig. 5 trajectories with different  $\chi$  are shown.

In Fig. 6 the quantity  $N_{Jacobi}$  of iterations with calculations of the Jacobi matrix versus the

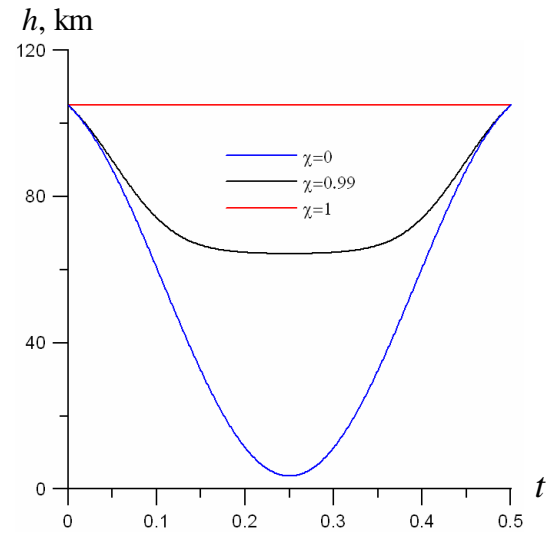


Fig. 5 Solutions for different homotopy parameter

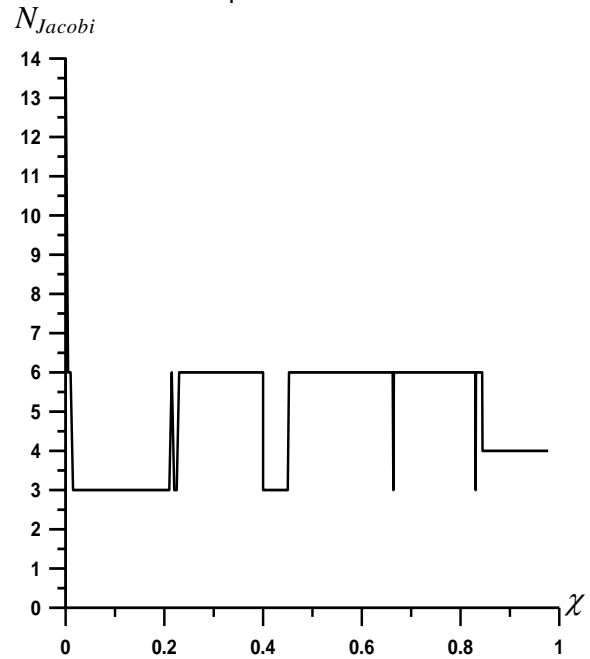


Fig. 6 The number of iteration  $N_{Jacobi}$  vs different homotopy parameter  $\chi$

homotopy parameter  $\chi$  is shown for the global extremal no. 1.

Note, the analytical solution for this extremal has a big altitude amplitude (Fig. 4), therefore the consumed mass for initial ( $\chi=0$ ) and final ( $\chi=1$ ) variants are differed in five orders. Nevertheless, the complex “ASTER” provided a regular convergence for solution of this problem.

**10 Analysis of extremals with the fuel mass consumption constraint**

The computation of optimal trajectories with constraints on the flight time and fuel mass consumption was provided according to the statement in Section 7. The Pontryagin maximum principle lets to reduce the optimization problem to the two-parametric boundary value problem. The last is solved by the program complex “ASTER”.

The obtained approximate optimal solutions are compared with the level cruise in Fig. 7. The right parts of optimal dependencies  $x_{f\max}(\Delta m, \tau = fix)$  related to the cross points are displayed lower than the line of the level flight due to different flight time on compared curves. The left parts of optimal dependencies  $x_{f\max}(\Delta m, \tau = fix)$  are higher than the line of the level flight. In the domain above the line for the level flight the maximal range (at the optimal trajectory) is more then the range of the level flight at the same mass consumption. The example of the optimal trajectory, which parameters correspond to the pink cross in Fig. 7, is shown in Fig. 8.

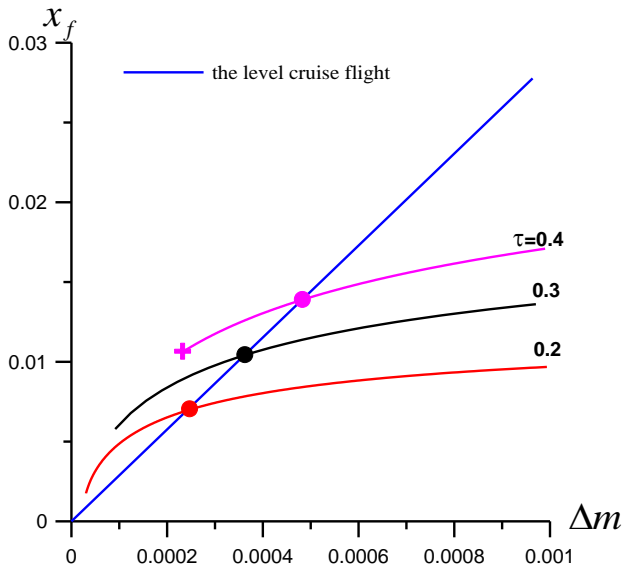


Fig. 7 Comparison of the optimal solutions with the level flight

The envelope of the family of functions  $x_{f\max}(\Delta m, \tau = fix)$  for a  $\tau$ -interval is the dependence of the maximal range on the fuel mass consumption with free flight duration.

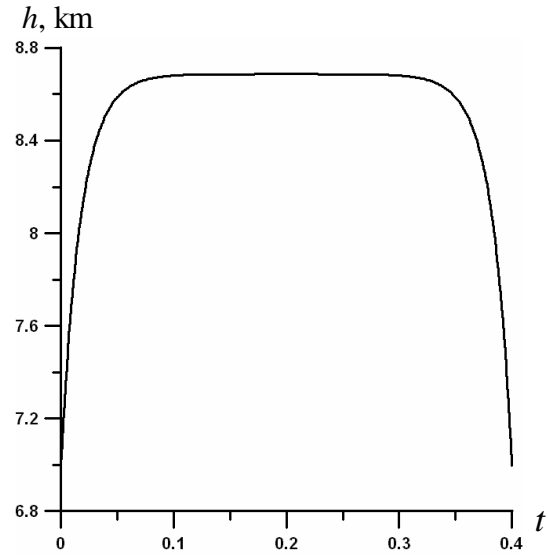


Fig. 8 The optimal trajectory with the range advantage to the level flight

**11 Analysis of aerodynamic loads at the extremals**

Let us return to the maximum range problem with the fixed flight time (see Section 4). It is shown in Fig. 4 that the oscillatory trajectories have the wide diapason of the altitude change. Since the constraints to the aerodynamic load factor were not considered it is necessary to ascertain that aerodynamic load factor is in reasonable limits. Using the analytical solutions (4.10) and (4.12) let us estimate the aerodynamic load factor at the extremal trajectories.

The normal aerodynamic load factor:

$$n_y = \frac{c_y q S}{m} . \tag{11.1}$$

From another side, according to Eq. (2.3):

$$n_y = w \dot{\nu} + \cos \nu , \tag{11.2}$$

where (see (4.17)):

$$\dot{\nu} = \frac{1}{H} . \tag{11.3}$$

Substituting (4.12) and (11.3) to (11.2) it is obtained:

$$n_y = 2 \cos \nu. \quad (11.4)$$

So the aerodynamic load factor at the optimal trajectories from (11.4) is:

$$|n_y| \leq 2.$$

Note that this result (for the used model of motion) is independent of aircraft characteristics.

## 12 Demonstration of advantage of oscillatory trajectories

Let us show advantage of oscillatory trajectories. Consider the local extremal no. 7 from the Section 5 in detail. The realizability of this trajectory is verified by numerical modeling of flight with more complete equations of motion (2.1) with the control that follows up the extremal. Although it is not the global optimal solution, but the gain in range in comparison with the level flight is significant: 18%. It has oscillatory character with altitude change of 14 km. It is achievable for maneuver aircrafts.

For example, consider aircraft which characteristics are given in the Appendix. The follow initial values are used:

$$v_i = 240 \text{ m/s}, h_i = 12800 \text{ m}.$$

The angle of attack and thrust are the control:

$$\begin{aligned} 0 \leq T \leq T_{\max}(v, h), \\ 0 \leq \alpha \leq 20^\circ. \end{aligned}$$

The ideal flight director system (FDS) that follows up the nominal trajectory (the extremal no. 7) is developed. The linear feedback control compensation is written as:

$$\begin{aligned} \alpha_{FDS} &= \alpha_{opt} + k_1(\gamma - \gamma_{opt}) + k_2(h - h_{opt}), \\ T_{FDS} &= T_{opt} + k_3(v - v_{opt}), \\ k_1 &= -200, k_2 = -10000, k_3 = -100, \end{aligned}$$

where  $\alpha_{opt}$  is determined by following for the extremal no. 7:

$$\alpha_{opt} = \frac{v_{opt} \dot{\gamma}_{opt} + g \cos \gamma_{opt}}{\frac{c_y^\alpha \rho v_{opt}^2 S}{2m}},$$

and  $T_{opt} = D(v, h)$  in according to assumptions of section 4. So the control variables are:

$$\begin{aligned} \alpha &= \begin{cases} \alpha_{FDS}, & 0 \leq \alpha_{FDS} \leq \alpha_{\max} \\ \alpha_{\max}, & \alpha_{FDS} > \alpha_{\max} \\ 0, & \alpha_{FDS} < 0 \end{cases}, \\ T &= \begin{cases} T_{FDS}, & 0 \leq T_{FDS} \leq T_{\max} \\ T_{\max}, & T_{FDS} > T_{\max} \\ 0, & T_{FDS} < 0 \end{cases}. \end{aligned} \quad (12.1)$$

Simulation of maneuver aircraft with real aerodynamic data and FDS (12.1) that follows up the extremal no. 7 is made. In Fig. 9 the comparison between the obtained trajectory and the nominal trajectory is shown.

The difference between the obtained trajectory and the nominal trajectory due to the

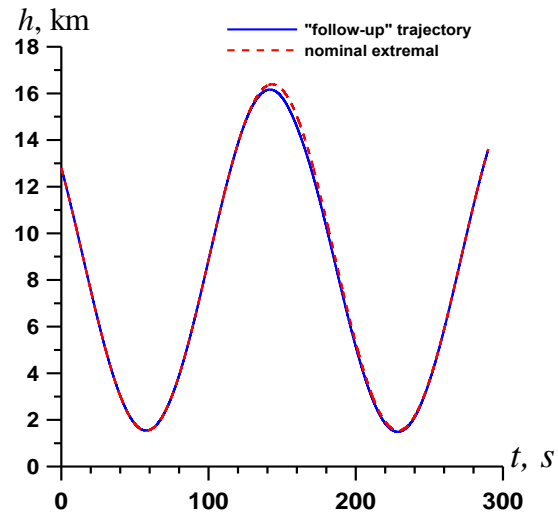


Fig. 9 Comparison of the nominal extremal with follow-up trajectory of maneuver aircraft with FDS

differences in physical models and constraints does not lead to significant changes in range. Mathematical simulation of aircraft motion with FDS confirms increment in range to 18% in comparison with the level flight. The program (12.3) ensures the expected gain in range with accuracy up to 1%.

### 13 Summary

The maximum range problem with the fixed flight time and fuel consumption is considered. Also the constraints to the altitude and velocity are taken into account. This problem is mutual to the minimum time-fixed fuel-fixed time problem and the minimum range-fixed time-fixed fuel problem.

In framework of the pseudo-conservative model the analytical solutions based on the Pontryagin maximum principle are obtained. All the local extremals that satisfy the necessary optimality conditions are obtained. They have the oscillatory character. The quantity of the extremals depends on parameters of problem. It is shown that the maximum range depends on generalized parameter.

It is proved that the aerodynamic load factor on the oscillatory trajectories:  $|n_y| \leq 2$ .

Analysis of realizability of the extremal on the complete equation of maneuver aircraft motion with the simplified flight director system is provided. The flight director system follows up the extremal that gives the gain 18% in range. The simulation includes real aerodynamic constraints on the angle of attack and thrust which are the control variables. A high accuracy in the range (up to 1%) of the analytical solutions with numerical simulation is shown.

For the maximum range problem with the given flight time and mass fuel consumption the numerical solutions are investigated by the continuation method with the analytical solutions as the first approximation.

### References

- [1] Pontryagin L.S., Boltyansky V.G., Gamkrelidze R.V. and Mischenko E.F. *The Mathematical Theory of Optimal Processes*. Interscience Publishers, New York, 1962.
- [2] Shkadov L.M., Bukhanova R.S., Illarionov V.F., Plokhikh V.P., *Mechanics of optimum three-dimensional motion of aircraft in the atmosphere*, NASA TTF-777, 1975.
- [3] Nguyen X. Vinh, *Flight mechanics of high-performance aircraft*. Cambridge University Press, 1993.
- [4] Franco A., Rivas D. and Valenzuela A. Minimum-fuel cruise at constant altitude with fixed arrival time, *Journal of Guidance, Control, and Dynamics*, Vol. 33, No. 1, 2010, pp. 280-285. doi: 10.2514/1.46465
- [5] Illarionov V.F., Pashincev V.T. Qualitative analysis of family of optimal trajectories in a problem of range maximization of aircraft flight. *Proceedings of TsAGI*, V. 1591, 1974.
- [6] Speyer J.L. Nonoptimality of the steady-state cruise for aircraft, *AIAA Journal*, vol. 14, No. 11, 1976, pp. 1604-1610.
- [7] Elmer G. Gilbert, Daniel T. Lyons, The improvement of aircraft specific range by periodic control, *AIAA, Guidance and Control Conference*, 1981, 10.2514/6.1981-1748
- [8] M.L. Shepard, K.D. Bilimoria, Optimization of aircraft cruise performance, *AIAA, 16th Atmospheric Flight Mechanics Conference*, 1989, 10.2514/6.1989-3386.
- [9] K.R. Suwal, E.M. Cliff, Singular, periodic solutions in aircraft cruise-dash optimization, *AIAA, Guidance, Navigation and Control Conference*, 1990, 10.2514/6.1990-3369.
- [10] Vinh N.X. *Optimal Trajectories in Atmospheric Flight*. Elsevier Scientific Publishing Co., Amsterdam, Holland, 1981.
- [11] Vinh N.X., Busemann A. and Culp R.D. *Hypersonic and Planetary Entry Flight Mechanics*. The University of Michigan Press, 1980.
- [12] Letov A.M., *Flight dynamic and control*, M.: Nauka, 1969 (in Russian)
- [13] Filatyev A.S. Optimization of Spacecraft Ascent Using Aerodynamic Forces, IAF-92-0022. *43rd Congress of the International Aeronautical Federation*, August 28-Sept. 5, 1992, Washington, DC.
- [14] Bryson A. E., Jr., and Ho Y. C., *Applied Optimal Control*, Wiley, New York, 1975.
- [15] Stechkin S.B., Subbotin, Yu.N., *Splines in the Computational Mathematics*, M.: Nauka, 1976 (in Russian).
- [16] Filatyev A.S., Yanova O.V. ASTER Program Package for the Thorough Trajectory Optimization. *41st AIAA «Guidance, Navigation & Control» Conference*, 6-9 August 2001, Montreal, Canada, AIAA-2001-4391.

## Appendix

Table 1. Dependence of angle of attack from lift coefficient

$\alpha$	0	2	4	6	8	10	12	14	16	18	20
$c_y$	0	0.17	0.35	0.52	0.7	0.86	0.99	1.09	1.16	1.21	1.28

Table 2 Dependence of thrust (kg) with afterburning from Mach number and altitude

M	<i>h, m</i>					
	0	3000	6000	9000	12000	15000
0.7	16800	12890	9200	6135	3583	1769
0.9	19100	14777	10900	7462	4783	2774
1.1	21400	17078	13100	94000	5922	3466
1.3	21000	19970	15500	11365	7804	5091
1.5	20760	21477	18454	13504	9865	6911
1.7	21000	21794	21000	15811	11859	8411
1.9	21116	21838	22030	18116	13744	9565
2.1	21079	21825	21938	20094	15385	10468
2.3	21000	21798	21500	21380	16628	11247
2.5	20971	21788	21330	21743	17379	12004

## Copyright Statement

The authors confirm that they, and/or their company or organization, hold copyright on all of the original material included in this paper. The authors also confirm that they have obtained permission, from the copyright holder of any third party material included in this paper, to publish it as part of their paper. The authors confirm that they give permission, or have obtained permission from the copyright holder of this paper, for the publication and distribution of this paper as part of the ICAS 2014 proceedings or as individual off-prints from the proceedings.